Anomalous transient behavior from an inhomogeneous initial optical vortex density

Filippus S. Roux

National Laser Centre, CSIR, P.O. Box 395, Pretoria 0001, South Africa (fsroux@csir.co.za)

Received December 9, 2010; revised February 11, 2011; accepted February 11, 2011;
posted February 14, 2011 (Doc. ID 139463); published March 22, 2011

Inhomogeneous optical vortex densities can be produced in stochastic optical fields by a combination of coherent and incoherent superposition of speckle fields. During subsequent propagation, the inhomogeneity in the vortex density decays away. However, the decay curves contain oscillatory features that are counterintuitive: for a short while, the inhomogeneity actually increases. We provide numerical simulations and analytic calculations to study the appearance of the anomalous features in the decay curves.

OCIS codes: 260.6042, 050.4865, 350.5500, 030.6600, 000.5490.

1. INTRODUCTION

The statistical properties of optical vortices in random optical fields have been studied by various authors [1–5]. Although this work includes monochromatic and nonmonochromatic, two-dimensional and three-dimensional, theoretical, numerical, and experimental work, it mostly focuses only on random (i.e., speckle) fields. As such, the vortex densities in these fields remain constant during propagation. Other kinds of stochastic optical fields differ from speckle fields in that their vortex densities undergo transient behavior. In general, such stochastic optical fields start from initial conditions that differ from that of a speckle field, and then during propagation this field eventually evolves into a beam with properties much like that of a speckle beam. Treating the propagation distance conceptually like a time axis, one can view this as a system evolving from some initial nonequilibrium state through some transient behavior to a final state that is in equilibrium.

Here, we consider such nonequilibrium stochastic optical fields. In particular, we are interested in the transient behavior of the optical vortex fields. Since this evolution happens during propagation of the optical beam through a linear medium, one may be led to believe that the transient behavior would be rather simple, perhaps just an exponential decay of the inhomogeneities that disturb the equilibrium until the homogeneity that represents the equilibrium state is restored. However, recently transients that contradict this simple behavior have been observed in numerical simulations [6]. These transients contain more structure than just exponential decay and, therefore, merit a deeper investigation.

For this purpose, we present in this paper the case of a nonequilibrium stochastic optical field that lends itself to both numerical simulation and analytical investigation. The latter is made possible by the fact that the initial conditions in this scenario can be expressed in terms of Gaussian random functions. As a result, one can use statistical optics methods [7] to analyze the evolution of the stochastic vortex field and compare the results with the results from the numerical simulations. The fact that one can study the evolution analytically provides more credibility of what has been observed in numerical simulations. It also allows a deeper investigation into the origin of the anomalous transient behavior. In particular, we are interested in the evolution of the vortex density, which is defined as the number of optical vortices (regardless of their topological charge) per unit area on the transverse plane perpendicular to the direction of propagation.

In this paper, we describe the experimental setup with which such a beam can be produced (Section 2). Then, we describe the numerical simulation in Section 3 for the evolution of this stochastic optical beam, and we show that it predicts anomalous transient behavior. Using a statistical optics method in Section 4, we compute the evolution of the vortex density for the same beam and show that it gives the same anomalous transient behavior. We investigate some of the properties of the vortex density evolution in Section 5 and end with some conclusions in Section 6.

2. EXPERIMENTAL SETUP

When a stochastic vortex field is produced by direct phase modulation of a plane wave, using a spatial light modulator or a diffractive optical element, the resulting beam directly behind the element does not have a Gaussian distribution. To perform statistical optics calculations for such a beam is challenging, because the simplifications that Gaussian statistics allow cannot be employed. The initial beam needs to have the properties of a speckle beam to allow the required simplifications that enables statistical optics calculations.

However, one can produce an optical beam with a nonuniform vortex density using speckle beams. The optical setup to produce such an inhomogeneous stochastic beam is shown in Fig. 1. The input beam is divided by a 50/50 beam splitter. The two resulting beams are each passed through a ground glass plate and spatially filtered (shown as circular apertures) to produce different sized speckles (hence, different vortex densities) in the two beams. The two beams are also mutually incoherent. Mach–Zehnder interferometers are used to produce sinusoidal interference patterns in each of the beams. The two beams are then (incoherently) recombined such that the dark bands of one interference pattern overlaps with the bright bands of the other. Because of the different vortex densities,

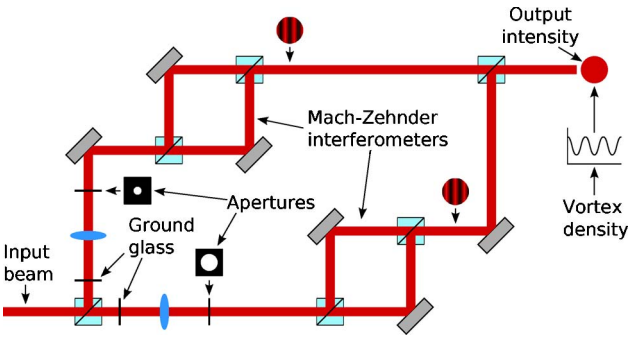

Fig. 1. (Color online) Setup to produce an inhomogeneous initial vortex density. It consists of two Mach–Zehnder interferometers that are used to produce interference patterns in two mutually incoherent speckle fields with different speckle sizes, which are then combined to give a sinusoidal variation in the vortex density.

the combined beam has a periodically varying vortex density and a constant average intensity.

The vortex density that is obtained at the output of this setup represents the initial state of the beam ψ_{in} at $z=0$. We now consider the subsequent evolution of the vortex density due to free-space propagation of this optical field. One can model the initial state of the optical field ψ_{in} as

$$\psi_{\text{in}}(x,y,z=0)=\psi_1(x,y)\sin(2\pi a_0 x)+\psi_2(x,y)\cos(2\pi a_0 x), \tag{1}$$

where $\psi_1(x,y)$ and $\psi_2(x,y)$ are speckle beams with different sized speckles and a_0 is the spatial frequency of the interference fringes. The two speckle beams can be expressed in terms of their spectra:

$$\psi_n(x,y)=\mathcal{F}^{-1}\{\tilde{\chi}_n(\mathbf{a})A_n(\mathbf{a})\} \qquad n=1,2, \tag{2}$$

where $\mathcal{F}^{-1}\{\cdot\}$ represents the inverse two-dimensional Fourier transform, $\mathbf{a}(=a\hat{x}+b\hat{y})$ is the two-dimensional transverse spatial frequency vector, $\tilde{\chi}_n(\mathbf{a})$ is a random complex function (Gaussian white noise) on the spatial frequency domain, and $A_n(\mathbf{a})$ is an aperture function or spectral envelope function with different widths for $n=1,2$, respectively. For computational convenience, we assume a Gaussian envelope:

$$A_n(\mathbf{a})=\frac{1}{W_n}\exp\left(\frac{-|\mathbf{a}|^2}{W_n^2}\right) \qquad n=1,2, \tag{3}$$

where W_n represents the width of the spectral envelope.

The random complex functions obey the following statistical properties:

$$\langle\tilde{\chi}_n(\mathbf{a})\rangle=\langle\tilde{\chi}_m(\mathbf{a}_1)\tilde{\chi}_n(\mathbf{a}_2)\rangle=\langle\tilde{\chi}_m^*(\mathbf{a}_1)\tilde{\chi}_n^*(\mathbf{a}_2)\rangle=0, \tag{4}$$

$$\langle\tilde{\chi}_m(\mathbf{a}_1)\tilde{\chi}_n^*(\mathbf{a}_2)\rangle=\Delta_a^2\delta_{mn}\delta(\mathbf{a}_1-\mathbf{a}_2), \tag{5}$$

for $m,n=1,2$, where Δ_a is the correlation width on the spectral domain.

The angular spectrum of the initial optical field (at $z=0$) is therefore given by

$$\begin{aligned}G_{\text{in}}(\mathbf{a})=&\frac{i\tilde{\chi}_1(a-a_0,b)}{W_1}\exp\left[\frac{-(a-a_0)^2-b^2}{W_1^2}\right]\\&-\frac{i\tilde{\chi}_1(a+a_0,b)}{W_1}\exp\left[\frac{-(a+a_0)^2-b^2}{W_1^2}\right]\\&+\frac{\tilde{\chi}_2(a-a_0,b)}{W_2}\exp\left[\frac{-(a-a_0)^2-b^2}{W_2^2}\right]\\&+\frac{\tilde{\chi}_2(a+a_0,b)}{W_2}\exp\left[\frac{-(a+a_0)^2-b^2}{W_2^2}\right]\end{aligned} \tag{6}$$

and the optical field at arbitrary z is obtained by Fresnel propagation of the initial optical field, which can be written as

$$\begin{aligned}g_{\text{in}}(x,y,z)=&\iint G_{\text{in}}(\mathbf{a})\exp[-i2\pi(ax+by)\\&+i\pi z\lambda(a^2+b^2)]\mathrm{d}a\mathrm{d}b,\end{aligned} \tag{7}$$

with λ being the wavelength.

3. NUMERICAL SIMULATION

In the numerical simulations, the input stochastic optical field [$\psi_{\text{in}}(x,y,z=0)$ in Eq. (1)] is represented by a sampled complex-valued function, consisting of an array of 512×512 samples, shown in Fig. 2. The random spectral functions $\tilde{\chi}_n(\mathbf{a})$ are generated as two-dimensional arrays of normally distributed complex values. The Fourier transform of the angular spectrum, produced according to Eq. (6), then gives an inhomogeneous speckle field with periodic boundary conditions. Hence, the resulting input stochastic optical field does not expand during propagation.

The free-space propagation of the input stochastic optical field is simulated with a numerical implementation of a Fourier optics-based beam propagation algorithm [8,9]. It propagates the initial stochastic optical field through free space over logarithmically increasing distances. At each point, the vortex distribution is determined by locating all the optical vortices inside the 512×512 sample window that represents the stochastic optical field at that propagation distance. A vortex extraction procedure is used that produces a 512×512 array of integers equal to 1 where vortices are located and zeros everywhere else. This array is regarded as a vortex density function. From these vortex distributions, one then extracts the specific spatial frequency components in which we are interested using a two-dimensional Fourier transform. In all the numerical simulations, the wavelength is chosen small enough to stay within the paraxial limit. The same simulation is

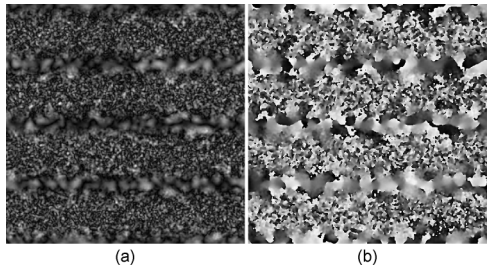

Fig. 2. Example of the (a) intensity and (b) phase of the initial optical field used in the numerical simulation, showing the variations of the speckle sizes and vortex density. The parameter values are $a_0=2$, $W_1=64$, and $W_2=16$.

repeated hundreds of times starting from different two-dimensional random arrays to produce averaged curves with standard deviations for the Fourier components.

The numerically simulated evolution of the vortex density defined in Eq. (1) is shown by the curves in Fig. 3. For this case, the parameter values are $a_0 = 2$, $W_1 = 64$, and $W_2 = 16$ in units defined by the sample spacing of the Fourier domain. The wavelength was selected to be equal to one sample spacing on the spatial domain.

Figure 3 shows, as a function of logarithmic propagation distance, three Fourier components: the global average vortex density $V(0)$, the fundamental spatial frequency (amplitude of the sinusoidal variations in the vortex density) $V(k_x)$, and the first harmonic $V(2k_x)$, where $k_x = 4\pi a_0$. The global average vortex density remains constant except for some relatively small transient variations. As expected, the fundamental spatial frequency component decays during propagation, but the decay curve contains some additional oscillations, colocated with the transients in the global average vortex density. The first harmonic remains close to zero, but also contains some variations that are colocated with those in the other two components.

The presence of the oscillations in the decay curve indicates that the transient behavior of this stochastic vortex field is more intricate than what one naively might have anticipated. Therefore, it qualifies as a case with anomalous transient behavior.

4. ANALYTICAL EVOLUTION

A benefit of producing the initial vortex density through the interference and incoherent superposition of speckle beams is that one can assume that the initial optical field has a Gaussian distribution. Therefore, one can employ statistical optics methods [7] to compute the evolution of the vortex density. Here, the random complex functions $\tilde{\chi}_n(\mathbf{a})$ have Gaussian distributions. We now use the properties of these random functions, as presented in Eqs. (4) and (5), to obtain the vortex density as a function of x and z—being one-dimensional, the vortex density remains independent of y. We closely follow the approach of [1,5] in our analysis.

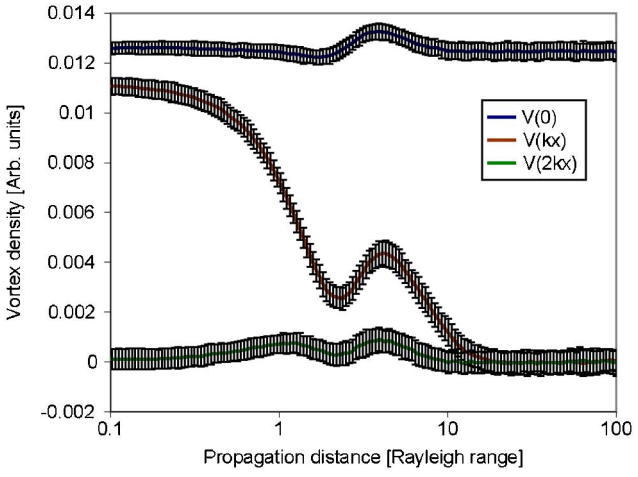

Fig. 3. (Color online) Numerically simulated evolution of an inhomogeneous vortex density, shown in terms of the Fourier coefficients $V(0)$, $V(k_x)$, and $V(2k_x)$, where $k_x = 4\pi a_0$, plotted as a function of logarithmic propagation distance. The curves are obtained from the average over hundreds of simulations with the error bars indicating the standard deviations.

The vortex density is obtained through local averaging of the number of first-order zeros in the optical field. One can define this average with the aid of an integration of the product of Dirac delta functions containing the real and imaginary parts of the optical field in their arguments. However, the gradients of the real and imaginary parts of the field are not orthogonal or equal to 1 at the locations of the vortices. Therefore, one needs to multiply the product of Dirac delta functions with the magnitude of the Jacobian determinant. The resulting expression for the vortex density in an arbitrary optical field over a small area A is then given by [1]

$$V_A = \frac{1}{A}\int_A \delta(\psi_r)\delta(\psi_i)|\partial_x\psi_r\partial_y\psi_i - \partial_x\psi_i\partial_y\psi_r|\mathrm{d}x\mathrm{d}y, \quad (8)$$

where ψ_r and ψ_i are, respectively, the real and imaginary parts of the optical field ψ.

It is more convenient to use additional Dirac delta functions to replace the derivatives of the real and imaginary parts in the Jacobian determinant with auxiliary integration variable. Each of the Dirac delta functions is now expressed in terms of its inverse Fourier transform. In compact notation, the resulting integral then has the form

$$V(\mathbf{x}) = \int \exp[i2\pi\mathbf{p}\cdot(\mathbf{q}-\tilde{\mathbf{U}})]|q_2q_5 - q_3q_4|\mathrm{d}^6p\mathrm{d}^4q|_{q_1=q_2=0}, \quad (9)$$

where $\mathbf{x}$ represents the three spatial coordinates (x, y, z),

$$\tilde{\mathbf{U}} = [\psi_r, \psi_i, \partial_x\psi_r, \partial_x\psi_i, \partial_y\psi_r, \partial_y\psi_i], \quad (10)$$

$$\mathbf{p} = [p_1, p_2, p_3, p_4, p_5, p_6], \quad (11)$$

$$\mathbf{q} = [q_1, q_2, q_3, q_4, q_5, q_6], \quad (12)$$

and the averaging over the small area A has been dropped. Note that q_1 and q_2 are actually superfluous and can be set equal to zero right from the start. However, for notational convenience we keep them until the end.

Because of the way in which the initial beam is formed, $\langle\psi_r\psi_i\rangle \neq 0$. For this reason, it is more convenient to work with the complex optical field and its complex conjugate, instead of the real and imaginary parts of the optical field. Therefore, we express the stochastic term in the exponent as

$$i2\pi\mathbf{p}\cdot\tilde{\mathbf{U}} = i\pi(\mathbf{P}^\dagger\tilde{\mathbf{W}} + \tilde{\mathbf{W}}^\dagger\mathbf{P}), \quad (13)$$

where

$$\mathbf{P} = \begin{bmatrix} p_1 + ip_2 \\ p_3 + ip_4 \\ p_5 + ip_6 \end{bmatrix} \quad \text{and} \quad \tilde{\mathbf{W}} = \begin{bmatrix} \psi \\ \psi_x \\ \psi_y \end{bmatrix}, \quad (14)$$

with $\psi_x = \partial_x\psi$, etc., and where the dot-product is now implicit in the notation.

Employing the properties of Gaussian distributions to evaluate part of the exponential function [7], one obtains

$$\langle \exp(-i2\pi \mathbf{p}\cdot\tilde{\mathbf{U}})\rangle = \exp(-\pi^2 \mathbf{P}^\dagger \langle \tilde{\mathbf{W}}\tilde{\mathbf{W}}^\dagger\rangle \mathbf{P}), \tag{15}$$

where

$$\langle \tilde{\mathbf{W}}\,\tilde{\mathbf{W}}^\dagger\rangle = \mathbf{M} = \begin{bmatrix} \langle \psi\psi^*\rangle & \langle \psi_x\psi^*\rangle & \langle \psi_y\psi^*\rangle \\ \langle \psi\psi_x^*\rangle & \langle \psi_x\psi_x^*\rangle & \langle \psi_y\psi_x^*\rangle \\ \langle \psi\psi_y^*\rangle & \langle \psi_x\psi_y^*\rangle & \langle \psi_y\psi_y^*\rangle \end{bmatrix}. \tag{16}$$

Thanks to Eq. (4), we have that $\langle \tilde{\mathbf{W}}\,\tilde{\mathbf{W}}^T\rangle = \langle \tilde{\mathbf{W}}^*\tilde{\mathbf{W}}^\dagger\rangle = 0$.

One can now evaluate the six Fourier integrals over $\mathbf{p}$ to obtain the probability density:

$$F(\mathbf{Q},\mathbf{Q}^\dagger) = \int \exp(i2\pi \mathbf{p}\cdot\mathbf{q} - \pi^2 \mathbf{P}^\dagger \mathbf{M}\mathbf{P})\mathrm{d}^6 p = \frac{\exp(-\mathbf{Q}^\dagger \mathbf{M}^{-1}\mathbf{Q})}{\pi^3 \det(\mathbf{M})}, \tag{17}$$

where

$$\mathbf{Q} = \begin{bmatrix} q_1 + iq_2 \\ q_3 + iq_4 \\ q_5 + iq_6 \end{bmatrix}. \tag{18}$$

The vortex density is then given by

$$V(\mathbf{x}) = \int F(\mathbf{Q},\mathbf{Q}^\dagger)|q_2 q_5 - q_3 q_4|\mathrm{d}^4 q|_{q_1=q_2=0}. \tag{19}$$

It remains now to compute the ensemble averages in Eq. (16) in order to obtain an expression for the probability density in Eq. (17). For this purpose, we use Eqs. (1)–(7) to calculate the ensemble averages for all the elements in $\mathbf{M}$ as a function of z. The only nonzero elements are

$$\langle \psi(\mathbf{x})\psi^*(\mathbf{x})\rangle = 2\pi + \pi C(x)[h_1(z) - h_2(z)], \tag{20}$$

$$\begin{aligned}\langle \psi_x(\mathbf{x})\psi^*(\mathbf{x})\rangle = {} & 2\pi^2 a_0 S(x)[(1 + i\pi z\lambda W_2^2)h_2(z) \\ & - (1 + i\pi z\lambda W_1^2)h_1(z)],\end{aligned} \tag{21}$$

$$\begin{aligned}\langle \psi_x(\mathbf{x})\psi_x^*(\mathbf{x})\rangle = {} & \pi^3[C(x)(4a_0^2 - T(z)W_2^2)h_2(z) \\ & - C(x)(4a_0^2 - T(z)W_1^2)h_1(z) \\ & + 8a_0^2 + W_1^2 + W_2^2],\end{aligned} \tag{22}$$

$$\langle \psi_y(\mathbf{x})\psi_y^*(\mathbf{x})\rangle = \pi^3[W_1^2 + W_2^2 + C(x)W_1^2 h_1(z) - C(x)W_2^2 h_2(z)], \tag{23}$$

where

$$T(z) = 1 - 4\pi^2\lambda^2 a_0^2 z^2, \tag{24}$$

$$C(x) = \cos(4\pi a_0 x), \tag{25}$$

$$S(x) = \sin(4\pi a_0 x), \tag{26}$$

$$h_n(z) = \exp(-2\pi^2\lambda^2 a_0^2 z^2 W_n^2). \tag{27}$$

Substituting the ensemble averages in Eqs. (20)–(23) with Eqs. (24)–(27) into Eq. (17), and using that in Eq. (19), one obtains the vortex density after evaluating the four q integrals. Finally, we obtain

$$\begin{aligned}V(\mathbf{x}) = {} & \frac{\pi\{W_1^2 + W_2^2 + C(x)[W_1^2 h_1(z) - W_2^2 h_2(z)]\}^{1/2}}{2\{2 + C(x)[h_1(z) - h_2(z)]\}^{3/2}}\{4[4 \\ & - [h_1(z) - h_2(z)]^2 \\ & - \pi^2\lambda^2(C(x)\{2 + C(x)[h_1(z) - h_2(z)]\}[W_1^4 h_1(z) \\ & - W_2^4 h_2(z)] + S(x)^2[W_1^2 h_1(z) - W_2^2 h_2(z)]^2)z^2]a_0^2 \\ & + \{2 + C(x)[h_1(z) - h_2(z)]\} \\ & \times \{W_1^2 + W_2^2 + C(x)[W_1^2 h_1(z) - W_2^2 h_2(z)]\}\}^{1/2}.\end{aligned} \tag{28}$$

We now use Eq. (28) to compute (numerically) the curves for the Fourier components that were considered in Fig. 3. The results of these calculations are compared with the results from the numerical simulation in Fig. 4. The numerical results are shown as discreet points with error bars and the analytical curves are shown as solid curves. Apart from a slight offset in the magnitude of the larger densities, the analytic curves follow the numerical curves precisely. The offset of approximately 4% is attributed to a small, but inevitable, inefficiency in the vortex extraction process that is used in the numerical simulations. Vortices in random optical fields can have any morphology (anisotropy), and when the vortices become too anisotropic, the numerical vortex extraction procedure fails to identify them as vortices. The statistical optics calculations and the numerical simulations are therefore in good agreement with each other.

5. PROPERTIES OF THE EVOLUTION

The initial vortex density at $z = 0$ [$h_1(0) = h_2(0) = 1$] is given by

$$\begin{aligned}V(\mathbf{x}) = {} & \frac{\pi}{4}\left\{1 + \frac{8a_0^2}{[W_1^2 + W_2^2 + C(x)(W_1^2 - W_2^2)]}\right\}^{1/2} \\ & \times [W_1^2 + W_2^2 + C(x)(W_1^2 - W_2^2)],\end{aligned} \tag{29}$$

which implies that the pure sinusoidal variation for the vortex density at $z = 0$ is only a good approximation if a_0 is small compared to $(W_1^2 + W_2^2)^{1/2}/8$.

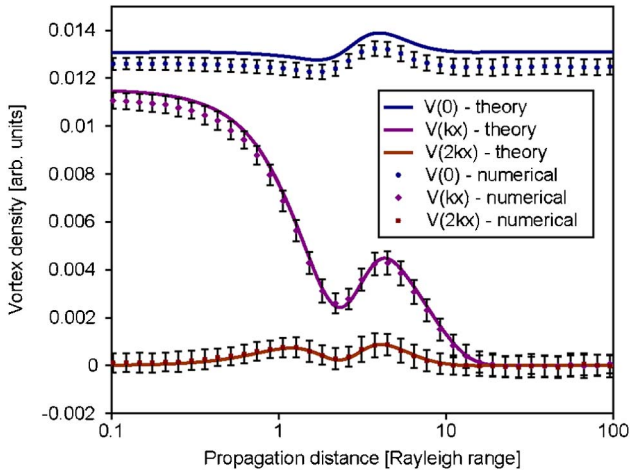

Fig. 4. (Color online) Comparison of the analytically calculated and numerically simulated evolution of an inhomogeneous optical vortex density, shown in terms of three Fourier coefficients of the optical vortex density function: the global average vortex density $V(0)$, the fundamental spatial frequency $V(k_x)$, and the first harmonic $V(2k_x)$, where $k_x = 4\pi a_0$. The numerical results are shown as discreet points representing the average values over several simulations with the error bars indicating the standard deviations. The solid curves represent the analytical results.

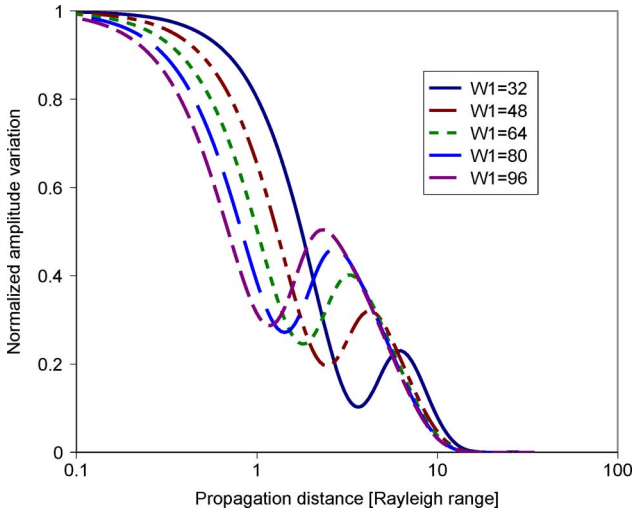

Fig. 5. (Color online) Curves of the normalized amplitude variation $\Delta V(z)$ for different values of W_1, with $W_2 = 16$ and $a_0 = 1$.

The equilibrium state is obtained in the limit $z \to \infty$ $[h_1(z) = h_2(z) \to 0]$ and is given by

$$V(\mathbf{x}) = \frac{\pi}{4}(W_1^2 + W_2^2)\left(1 + \frac{8a_0^2}{W_1^2 + W_2^2}\right)^{1/2}, \tag{30}$$

which corresponds to the initial vortex density with $C(x) = 0$.

Next, we determine how the anomalous oscillations depend on the three parameters a_0, W_1, and W_2. Provided that a_0 is small compared to W_0 and W_1, one can see from Eqs. (27) and (28) that a_0 only serves to scale z. Within the small a_0 limit, the amplitude of the anomalous oscillation is therefore invariant to the value of a_0.

We focus on the amplitude of the x variation as an indication of the anomalous oscillations. For this purpose we compute the difference between $V(\mathbf{x})$ for $C(x) = 1$ and $C(x) = -1$. The small a_0 limit is applied by expanding the latter result to subleading order a_0, and then the result is normalized with respect to its value at $z = 0$. This leads to the following expression:

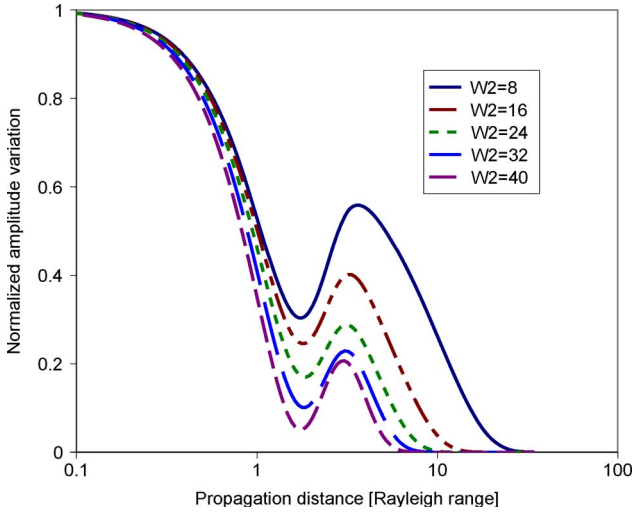

Fig. 6. (Color online) Curves of the normalized amplitude variation $\Delta V(z)$ for different values of W_2, with $W_1 = 64$ and $a_0 = 1$.

$$\Delta V(z) = \frac{2[h_1(z) + h_2(z)]}{4 - [h_1(z) - h_2(z)]^2} - 8a_0^2\left(\frac{\pi^2\lambda^2 z^2[W_1^4 h_1(z) - W_2^4 h_2(z)] + 2[h_1(z) - h_2(z)]}{\{4 - [h_1(z) - h_2(z)]^2\}(W_1^2 - W_2^2)}\right). \tag{31}$$

In Figs. 5 and 6, we plot $\Delta V(z)$ for various values of W_1 and W_2, respectively. In Fig. 5, we see that, for larger values of W_1, the amplitude of the anomalous oscillation grows larger with larger average vortex density, and the oscillation shifts to smaller propagation distances and it also extends over slightly larger ranges of propagation distance. On the other hand, in Fig. 6, we see that the amplitude of the anomalous oscillation grows smaller for larger values of W_2 and the average vortex density at the oscillations also becomes smaller, but these anomalous oscillations remain more or less at the same propagation distances, while spreading out over a wider range of propagation distances.

6. CONCLUSIONS

Perhaps the most pertinent observation is the fact that, thanks to the agreement between analytical and numerical results, the anomalous transient behavior is a physical effect and not just a numerical artifact. Nevertheless, it would be worthwhile to reproduce these results in an experimental setup. Although the setup itself is not too difficult, the observation of the vortex distribution over logarithmically increasing distances may present some challenges.

The only way in which the initial optical field differs from a speckle field is the correlations that exist in the initial field. These correlations are responsible for setting up the initial variation in the vortex density, and they are also responsible for the anomalous transient behavior. Apart from these correlations, there is no observable difference between this optical field and a homogeneous speckle field. In fact, the scintillation index (given by $\langle I^2\rangle/\langle I\rangle^2 - 1$, where I is the intensity), which is always equal to 1 for a speckle field, is also equal to 1 for the stochastic optical field that we consider here. The unity scintillation index is a clear indication that the Gaussian distribution of the stochastic optical field remains the same over all propagation distances. One can only observe the nonequilibrium behavior of this stochastic optical field by looking at the vortex density (or the speckle sizes), as shown in Fig. 2.

The propagation-dependent evolution of the vortex density derives from the propagation-dependent correlation functions in Eqs. (20)–(23). Viewed as a stochastic process, this beam is not stationary and therefore also not ergodic even though it is constructed out of speckle fields that are ergodic. In fact, the only reason for the loss of ergodicity/stationarity lies in the lateral correlations that are produced in the initial optical field. As far as the author knows, this is the first proposal of such an optical field.

The correlation functions in Eqs. (20)–(23) are computed as ensemble averages. Because of the loss of ergodicity, these correlation functions cannot be computed as time (or spatial) averages. In fact, the autocorrelation function of the beam profile of a deterministic optical beam propagating through free space is independent of the propagation distance. This follows immediately from the Wiener–Khintchine theorem, which states that the autocorrelation function is the Fourier transform of the power spectral density. Being the modulus

squared of the angular spectrum, the latter does not depend on the propagation distance. As a result, the correlation functions that one would compute for a single instance of the stochastic optical field under consideration would be independent of propagation distance even though the vortex density evolves as a function of propagation distance.

The experimental setup proposed here can be modified to produce a different initial stochastic optical field. One can, for instance, introduce a relative tilt between the overlapping interference patterns. The effect would be to create a nonuniform topological charge density. In this way, one would be able to investigate the evolution of inhomogeneous topological charge densities using statistical optics.

REFERENCES

1. M. V. Berry, "Disruption of wavefronts: statistics of dislocations in incoherent Gaussian random waves," J. Phys. A: Math. Gen. **11**, 27–37 (1978).
2. I. Freund, N. Shvartsman, and V. Freilikher, "Optical dislocation networks in highly random media," Opt. Commun. **101**, 247–264 (1993).
3. I. Freund, "Optical vortices in Gaussian random wave fields: statistical probability densities," J. Opt. Soc. Am. A **11**, 1644–1652 (1994).
4. N. Shvartsman and I. Freund, "Vortices in random wave fields: nearest neighbor anticorrelations," Phys. Rev. Lett. **72**, 1008–1011 (1994).
5. M. V. Berry and M. R. Dennis, "Phase singularities in isotropic random waves," Proc. R. Soc. London A **456**, 2059–2079 (2000).
6. M. Chen and F. S. Roux, "Evolution of the scintillation index and the optical vortex density in speckle fields after removal of the least-squares phase," J. Opt. Soc. Am. A **27**, 2138–2143 (2010).
7. J. W. Goodman, *Statistical Optics* (Wiley, 1985).
8. A. J. Devaney and G. C. Sherman, "Plane-wave representations for scalar wave fields," SIAM Rev. **15**, 765–786 (1973).
9. J. W. Goodman, *Introduction to Fourier Optics*, 2nd ed. (McGraw-Hill, 1996).